Available online at www.sciencedirect.com
ScienceDirect
Journal of Power Sources 171 (2007) 948–952
JOURNAL OF POWER SOURCES
www.elsevier.com/locate/jpowsour

Short communication

Solvothermal synthesis and ex situ XRD study of nano-Ni_3Sn_2 used as an anode material for lithium-ion batteries

Haiying Qin, Xinbing Zhao, Nianping Jiang, Zhoupeng Li *

College of Materials Science and Chemical Engineering, Zhejiang University, Hangzhou 310027, China

Received 29 January 2007; received in revised form 21 May 2007; accepted 26 May 2007
Available online 6 June 2007

Abstract

Nano-Ni_3Sn_2 intermetallic compound was successfully prepared by solvothermal method for an anode material of lithium-ion batteries. Its microstructure was characterized by X-ray diffraction (XRD), field emission scanning electron microscopy (FESEM) and transmission electron microscopy (TEM). Electrochemical performances were evaluated in a lithium-ion model cell Li/$LiPF_6$ (EC + DMC)/Ni_3Sn_2. The electrochemical lithiation and de-lithiation behavior of nano-Ni_3Sn_2 was investigated by ex situ XRD. Diffraction peaks of Ni_3Sn_2 widened and shrank gradually during lithiation. Sharp Ni_3Sn_2 peaks appeared again after full de-lithiation. It was proved that nano-Ni_3Sn_2 could be reversibly charged and discharged with lithium though the de-lithiation capacity of nano-Ni_3Sn_2 was lower than its theoretical capacity.

Keywords: Lithium-ion battery; Anode; Ni_3Sn_2; Solvothermal synthesis; Ex situ XRD

1. Introduction

Recently, many studies have been focused on lithium storage alloys since Fuji photo film company issued a patent on tin-based amorphous composite oxides (TCO) as novel anode materials for lithium-ion batteries in 1996 [1]. Compared with the carbonaceous materials, lithium storage alloys showed large capacity but low reversible capacity. It was reported that the cycling performance of tin could be significantly improved by secondary component addition to form intermetallic compounds such as Sn_2Fe [2], Sn_2FeC [3], Cu_6Sn_5 [4,5], Ni_xSn [6].

Ni–Sn intermetallic compounds were studied due to their high theoretical capacities and excellent cycling properties. Many synthesis methods of Ni–Sn intermetallic compounds have been developed, such as ball milling [6–8], sintering [9], E-beam evaporating [10], reductive precipitation [11] and electroplating [12–14]. Recently, Kim et al. [10] synthesized Ni_3Sn_2 powders with average grain sizes of 15 and 73 nm by mechanical alloying. However, their capacities (around 30 mAh g^{-1}) were much lower than its theoretical capacity (570 mAh g^{-1}). Similar results have been reported by Ehrlich [6].

Since the melting point of Sn is much lower than that of Ni, it is difficult to prepare Ni–Sn alloys with well-proportioned component by Arc-melting or sintering. Mechanical alloying was considered to be a suitable method to prepare Ni–Sn alloy, but Ni_3Sn_2 showed negative results [6,10]. Besides mechanical alloying, solvothermal method was considered as a promising way for synthesis of homogeneous nano-sized materials [15]. It was thought that the sample synthesized by solvothermal method would be more homogeneous than that synthesized by mechanical alloying. It was expected that the Ni_3Sn_2 could reach to a higher capacity by using solvothermal method to prepared Ni_3Sn_2. In this paper, the temperature effect on Ni_3Sn_2 formation was investigated. The microstructure was characterized by X-ray diffraction (XRD), field emission scanning electron microscopy (FESEM) and transmission electron microscopy (TEM). Ex situ XRD was used to characterize the electrochemical lithiation and de-lithiation behavior of the nano-Ni_3Sn_2. The electrochemical reaction mechanism of Ni_3Sn_2 anode was discussed based on experimental results.

2. Experimental details

Nano-Ni_3Sn_2 powders were prepared at different temperatures by solvothermal method. $SnCl_2{\cdot}2H_2O$ (0.02 mol),

* Corresponding author. Tel.: +86 571 87951977; fax: +86 571 87953149.
E-mail address: zhoupengli@zju.edu.cn (Z. Li).

0378-7753/$ – see front matter © 2007 Elsevier B.V. All rights reserved.
doi:10.1016/j.jpowsour.2007.05.097

$NiCl_2{\cdot}6H_2O$ (0.03 mol) and $NaBH_4$ (0.1 mol) were put into a Teflon-coated autoclave in which anhydrous ethanol (150 ml) has been filled. The autoclave was maintained at a certain temperature for 24 h, and then was cooled down to room temperature. The precipitate was filtered, washed with anhydrous ethanol and distilled water in sequence, then dried at 110 °C under vacuum for 12 h. The result of differential scanning calorimetry (DSC) showed that there was no sample oxidation happened during drying under vacuum. The product yield (obtained amount/expected amount) was around 48% according to the calculation from reaction (1).

The sample structure was identified by powder XRD with Rigaku-D/MAX-2550PC diffractometer using Cu Kα radiation (λ = 1.5406 Å). The morphology was observed with a Philips-FEI Sirion 200 field emission scanning electron microscopy and JEM-200CX transmission electron microscopy.

Test electrodes were prepared by coating the slurry of anode materials on copper foil. The slurry was composed of Ni_3Sn_2 powders (80 wt.%), acetylene black (10 wt.%) as conducting agent, and poly(vinylidene fluoride) (PVDF) (10 wt.%) as a binder in 1-methyl-2-pyrrolidinone. Cells were assembled in an Ar-filled glove box. A metallic lithium foil was used as a counter electrode. The electrolyte solution was composed of 1 M $LiPF_6$ in ethylene carbonate (EC)/dimethyl carbonate (DMC) (1:1 ratio in volume). Anode and cathode were separated by a polypropylene (PP) micro porous membrane. Cells were galvanostatically cycled at a constant current density of 20 mAg^{-1} between 0.05 and 2 V versus lithium. Cyclic voltammograms have been recorded between 0.05 and 2 V with a scanning rate of 0.1 mV s^{-1} at room temperature on an Arbin-001 *MITS* 2.9-BT2000 instrument.

To investigate the lithiation and de-lithiation behavior of Ni_3Sn_2, ex situ XRD patterns of Ni_3Sn_2 electrodes were collected at selected voltage points during charge and discharge processes. Model batteries were dismantled in an Ar-filled glove box and electrode samples were sealed with Vaseline to avoid air exposure. Samples were immediately transferred to the analysis chamber of the XRD apparatus. Data were collected from 25° to 80° of 2θ with step of 0.02°.

3. Results and discussion

3.1. Preparation and characterization of nano-Ni_3Sn_2

XRD patterns of samples along with standard XRD patterns of Ni_3Sn_2, $NiCl_2{\cdot}6H_2O$ and $SnCl_2{\cdot}2H_2O$ are shown in Fig. 1. It was found that peaks of $SnCl_2{\cdot}2H_2O$, $NiCl_2{\cdot}6H_2O$ disappeared but Ni_3Sn_2 peaks appeared after heating the mixture of $SnCl_2{\cdot}2H_2O$, $NiCl_2{\cdot}6H_2O$ and $NaBH_4$. Ni_3Sn_2 was formed even at 150 °C, though some metallic Sn existed. With increasing the reaction temperature, Sn disappeared and Ni_3Sn_2 peaks became clear and strong. The XRD result strongly proved that the Ni_3Sn_2 compound was formed at 240 °C.

According to the addition amount of $SnCl_2{\cdot}2H_2O$ (0.02 mol), $NiCl_2{\cdot}6H_2O$ (0.03 mol) and $NaBH_4$ (0.1 mol), the following reaction was suggested:

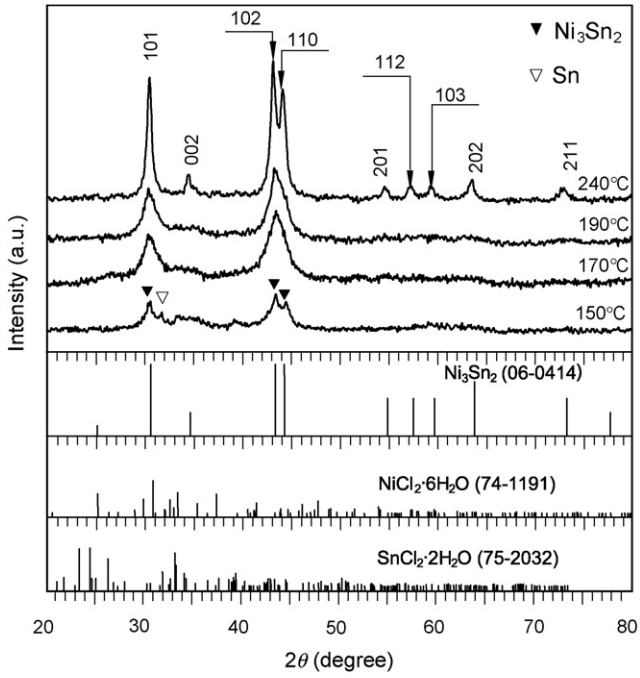

Fig. 1. XRD patterns of Ni_3Sn_2 samples prepared by solvothermal method at different temperatures.

$$2SnCl_2 + 3NiCl_2 + 10NaBH_4 \rightarrow Ni_3Sn_2 + 10NaCl + 5B_2H_6 + 5H_2 \quad (1)$$

Powders prepared by solvothermal method at 240 °C were agglomerated with small granules with particle size below 30 nm as shown in Fig. 2a. These irregular particles were loosely connected to form a network structure as shown in Fig. 2b. According to the Dehye–Sherrer equation of peak width versus grain size, the average grain size was estimated to be around 25.3 nm.

3.2. Electrochemical properties of nano-Ni_3Sn_2

Charge (lithiation) and discharge (de-lithiation) profiles in the first three cycles of the nano-Ni_3Sn_2 electrode are shown in Fig. 3. The lithiation capacity of the first cycle reached up to 380 mAh g^{-1} but the de-lithiation capacity fell down to 136 mAh g^{-1}. The occurrence of this irreversible capacity can be attributed to formation of a thin film resulted from a catalytic decomposition of electrolyte [16,17]. The following charge curve indicated that the lithiation capacity of nano-Ni_3Sn_2 was 150 mAh g^{-1}. This result demonstrated that the lithium could reversibly insert and emerge from nano-Ni_3Sn_2 although the capacity was lower than its theoretical capacity of 570 mAh g^{-1}.

In order to understand the electrochemical behavior of nano-Ni_3Sn_2 anode during lithiation and de-lithiation cycles, the cycle voltammetry (CV) of Ni_3Sn_2 anodes has been analyzed. Results are shown in Fig. 4. It was found that one compound was irreversibly formed at 1.1 V (point b), another two compounds were reversibly formed at 0.5 V (point d) and 0.05 V (point f) versus

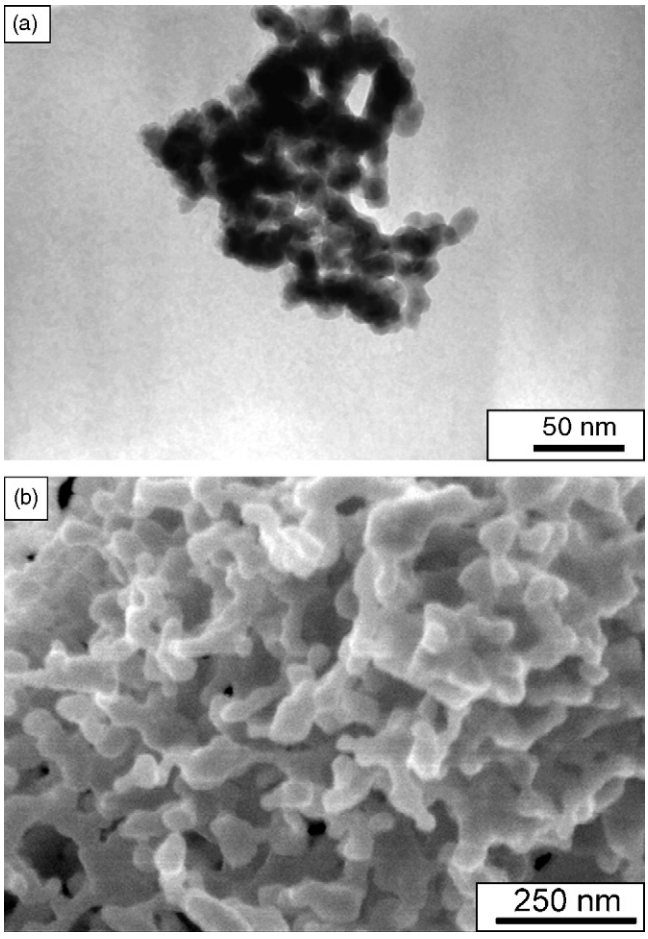

Fig. 2. TEM (a) and FESEM (b) images of Ni_3Sn_2 powders prepared by solvothermal method.

Li (1 M $LiPF_6$ in EC/DMC) in first charge process. This result was coincident with the former result obtained from galvostatic charge and discharge cycling. As shown in Fig. 4, Li was de-lithiated by two steps at 0.65 and 1.15 V, respectively, which

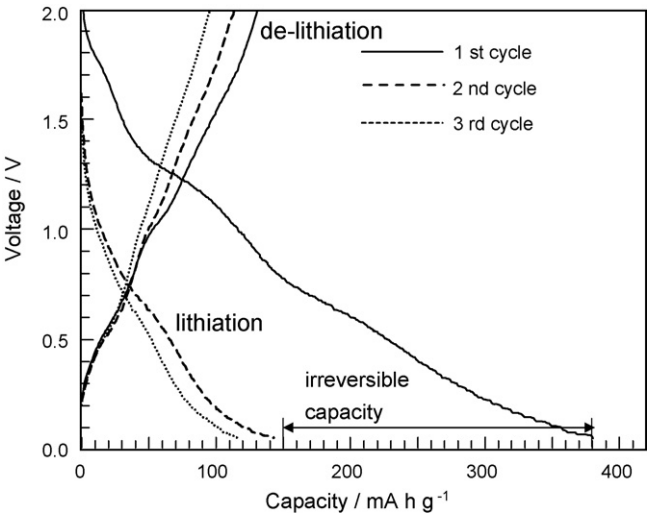

Fig. 3. Charge–discharge curves of nano-Ni_3Sn_2 electrode at a current density of 20 mAg^{-1}.

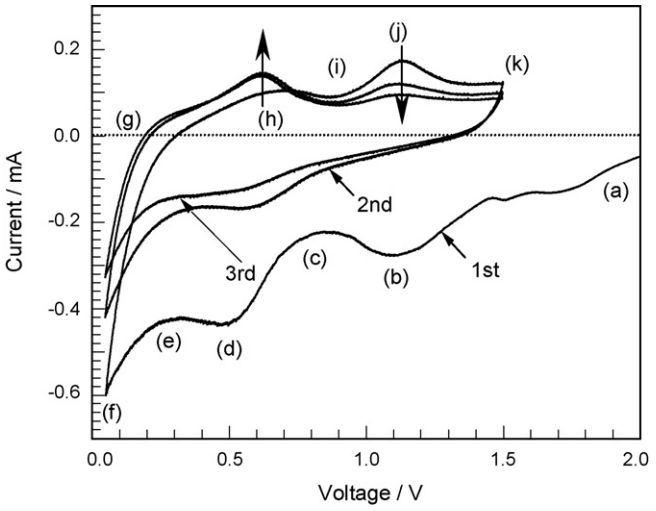

Fig. 4. Cyclic voltammetry curves of the Ni_3Sn_2 electrode.

indicated that lithium emerged from Ni_3Sn_2 electrode in two chemical states. It was interesting to note that the intensity of peaks located at 0.65 V increased at the same time in the next two cycles, but the intensity of peaks located at 1.15 V decreased. This result indicated that the de-lithiation process might have a dynamic change between two chemical states. More detailed researches are needed to explain the Li insert and emergence behavior at different chemical states.

3.3. Lithiation and de-lithiation mechanism of nano-Ni_3Sn_2

In order to understand the lithiation and de-lithiation behavior in nano-Ni_3Sn_2, ex situ XRD analyses were conducted during lithiation and de-lithiation cycling at selected cell voltages. Fig. 5 shows the ex situ XRD data (2θ from 25° to 80°) collected from points (a) to (k) as marked in Fig. 4. Main XRD peaks of initial Ni_3Sn_2 were located at 31°, 43° and 44° in 2θ. The original intention of this test was to find evidences to prove that lithium reacted reversibly with Ni_3Sn_2 to form Li–Sn alloys during lithiation as suggested by Lee et al. [7]. However, the peaks of Li–Sn alloys were failed to be distinguished by XRD. Diffraction peaks of Ni_3Sn_2 gradually widened and shrank during lithiation from points (a) to (f). It means that the alloy crystallinity was decreased during lithiation as suggested by Mukaibo et al. [14]. It was believed that the reversible lithiation capacity of 150 $mAh\,g^{-1}$ was the actual capacity of nano-Ni_3Sn_2 according to the result of galvanostatic cycle profile. Then the x in $Li_xNi_3Sn_2$ was 2.3.

The ex situ XRD data of the de-lithiation process from points (f) to (k), showed that peaks at 31°, 43° and 44° in 2θ gradually became evidently. The emergence of the sharp Ni_3Sn_2 peaks indicated that Ni_3Sn_2 was formed again when lithium fully emerged from $Li_xNi_3Sn_2$.

Based on the results and discussion above, it is reasonable to suggest that Ni_3Sn_2 electrochemically reacted with Li through following mechanism.

The Ni_3Sn_2 crystallinity was decreased due to formation of $Li_{2.3}Ni_3Sn_2$ during lithiation process. The $Li_{2.3}Ni_3Sn_2$ with low

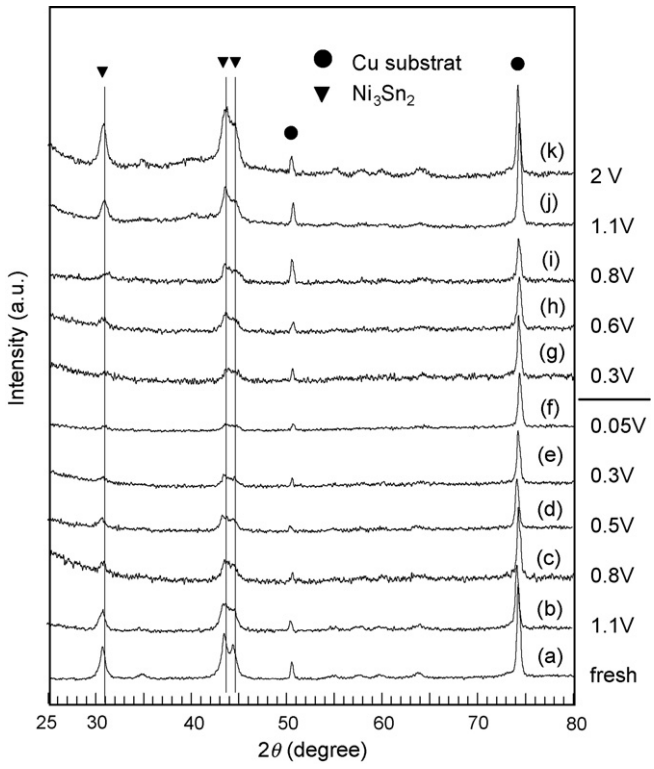

Fig. 5. Ex-XRD patterns evolution of Ni_3Sn_2 electrodes during lithiation and de-lithiation.

crystallinity then released Li^+ ion and crystalline Ni_3Sn_2 structure was reconstructed during de-lithiation process.

Comparing with Ni_3Sn_2 prepared by mechanical alloying [6,10], the sample prepared by solvothermal method showed a higher capacity. However, the experimental capacity of Ni_3Sn_2 was still lower than its theoretical capacity. In order to find out the reasons for this low experimental capacity, we made a comparison of the first de-lithiation capacities of Ni–Sn alloys [7–10,12,14,18–21] with their theoretical capacities and formation enthalpies (per mole of Sn) as shown in Fig. 6. It was found that not only the Ni_3Sn_2 but also Ni_3Sn_4 exhibited much lower de-lithiation capacity than their theoretical capacities.

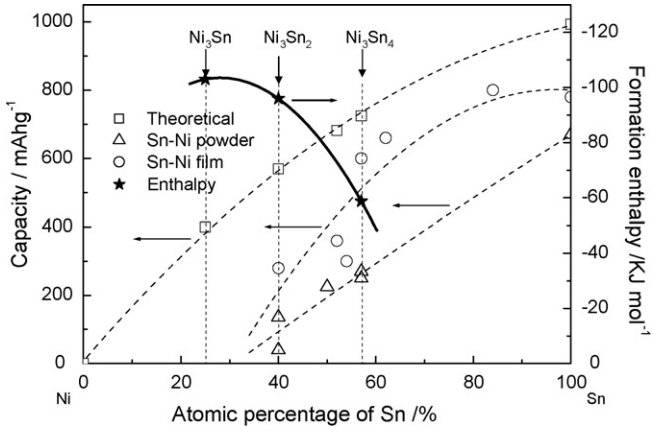

Fig. 6. Comparison of the first de-lithiation capacities, theoretical capacities and alloy formation enthalpy of Ni–Sn alloys.

With decreasing the atomic percentage of tin in Ni–Sn alloys, theoretical capacity and experimental capacity were decreased simultaneously but alloy formation enthalpy was increased.

There is a well-known rule that was called *rule of reversed stability* [22] in metal hydride thermodynamics. The higher the alloy formation enthalpy, the more stable the alloy. Hydrogen is difficult to be absorbed into a stable alloy with large alloy formation enthalpy. It was thought that lithium storage alloy was similar to hydrogen storage alloy. It can be expected that lithium atoms would more difficultly insert into a more stable alloy. Considering that the formation enthalpy of Ni_3Sn_2 was higher than that of Ni_3Sn_4, it can be understood that the capacity of Ni_3Sn_2 was lower than that of Ni_3Sn_4 due to the higher alloy stability of Ni_3Sn_2. From Fig. 6, it can be seen that the experimental capacities of Ni–Sn alloys were lower than their theoretical capacities. Furthermore, anodes made of alloy powders usually showed lower capacities than that made of alloy films. It is known that alloy films usually have higher electric conductivity than alloy powders. It implied that the electric conductivity of electrodes played an important role in lithiation and de-lithiation processes. Therefore, the low capacity of Ni_3Sn_2 in our experiments was caused by its higher alloy stability and the poor electronic conductivity of the anode. How to decrease the alloy stability by element substitution, and how to improve the electric conductivity of Ni–Sn alloy anode will be our next tasks to reach up a higher capacity. As a suggestion, we think that partial substitution of Ni with Al in Ni_3Sn_2 might improve the lithium storage capacity because Al substitution effect has been proved in hydrogen storage material of Ni–H batteries [23] and Al is a good anode material for lithium-ion batteries [24]. Electrodeposition might be an effective way to improve the electronic conductivity by formation of 3-dimention macroporous Ni–Sn alloy electrodes as suggested by Kea et al. [25].

4. Conclusions

Nano-Ni_3Sn_2 intermetallic compound was successfully synthesized by solvothermal method in ethanol solution at 240 °C. Comparing with Ni_3Sn_2 prepared by mechanical alloying, Ni_3Sn_2 prepared by solvothermal method showed a higher capacity (136 mAh g^{-1}). Ni_3Sn_2 can react with lithium reversibly though de-lithiation capacity of nano-Ni_3Sn_2 ($Li_{2.3}Ni_3Sn_2$) was lower than its theoretical capacity ($Li_{8.8}Ni_3Sn_2$). This low capacity of Ni_3Sn_2 was caused by its higher alloy stability and poor electronic conductivity of Ni_3Sn_2 powders.

Acknowledgments

This work is financially supported by Hi-tech Research and Development Program of China (863), grant no. 2006AA05Z120.

References

[1] Y. Idota, T. Kubota, A. Matsufuji, Y. Maekawa, T. Miyasaka, Science 276 (5317) (1997) 1395.

[2] O. Mao, J.R. Dahn, J. Electrochem. Soc. 146 (2) (1999) 414.
[3] O. Mao, R.A. Dunlap, J.R. Dahn, J. Electrochem. Soc. 146 (2) (1999) 405.
[4] K.D. Kepler, J.T. Vaughey, M.M. Thackeray, Electrochem. Solid State Lett. 2 (7) (1999) 307.
[5] D. Larcher, L.Y. Beaulieu, D.D. MacNeil, J.R. Dahn, J. Electrochem. Soc. 147 (5) (2000) 1658.
[6] G.M. Ehrlich, C. Durand, X. Chen, T.A. Hugener, F. Spiess, S.L. Suib, J. Electrochem. Soc. 147 (3) (2000) 886.
[7] H.Y. Lee, S.W. Jang, S.M. Lee, S.J. Lee, H.K. Baik, J. Power Sources 112 (1) (2002) 8.
[8] I. Amadei, S. Panero, B. Scrosati, G. Cocco, L. Schiffini, J. Power Sources 143 (1–2) (2005) 227.
[9] J.H. Ahn, G.X. Wang, J. Yao, H.K. Liu, S.X. Dou, J. Power Sources 119 (2003) 45.
[10] Y.L. Kim, H.Y. Lee, S.W. Jang, S.J. Lee, H.K. Baik, Y.S. Yoon, Y.S. Park, S.M. Lee, Solid State Ionics 160 (3–4) (2003) 235.
[11] Q.F. Dong, C.Z. Wu, M.G. Jin, Z.C. Huang, M.S. Zheng, J.K. You, Z.G. Lin, Solid State Ionics 167 (1–2) (2004) 49.
[12] O. Crosnier, T. Brousse, X. Devaux, P. Fragnaud, D.M. Schleich, J. Power Sources 94 (2) (2001) 169.
[13] H. Mukaibo, T. Momma, M. Mohamedi, T. Osaka, J. Electrochem. Soc. 152 (3) (2005) A560.
[14] H. Mukaibo, T. Osaka, T. Momma, J. Power Sources 146 (1–2) (2005) 457.
[15] J. Xie, X.B. Zhao, G.S. Cao, Y.D. Zhong, M.J. Zhao, J.P. Tu, Electrochim. Acta 50 (9) (2005) 1903.
[16] N. Tamura, R. Ohshita, M. Fujimoto, S. Fujitani, M. Kamino, I. Yonezu, J. Power Sources 107 (1) (2002) 48.
[17] L.Y. Beaulieu, S.D. Beattie, T.D. Hatchard, J.R. Dahn, J. Electrochem. Soc. 150 (4) (2003) A419.
[18] X.Q. Cheng, P.F. Shi, J. Alloy. Compd. 391 (1–2) (2005) 241.
[19] M. Inaba, T. Uno, A. Tasaka, J. Power Sources 146 (1–2) (2005) 473.
[20] N. Pereira, L.C. Klein, G.G. Amatucci, Solid State Ionics 167 (1–2) (2004) 29.
[21] J. Hassoun, S. Panero, B. Scrosati, J. Power Sources 160 (2) (2006) 1336.
[22] H.H. van Mal, K.H.J. Buschow, A.R. Miedema, J. Less-Common Met. 35 (1974) 65.
[23] J. Guo, R. Zhang, W.-q. Jiang, G.-x. Li, W.-l. Wei, J. Alloy. Compd. 429 (1–2) (2007) 348.
[24] M. Winter, J.O. Besenhard, M.E. Spahr, P. Novak, Adv. Mater. 10 (10) (1999) 725.
[25] F.-s. Ke, L. Huang, H.-h. Jiang, H.-b. Wei, F.-z. Yang, S.-g. Sun, Electrochem. Commun. 9 (2) (2007) 228.